

# Chapter 1

## INTRODUCTION

The work in this thesis focuses on the light motion in the galactic halo, which includes deflection and lensing properties in various physical scenarios including wormholes. Two special ingredients are to be noted. First one is the Rindler-Ishak method [1], which is the tool used here for the calculation of light deflection as it can handle both asymptotically flat and *non-flat* spacetimes. As a test of the validity of the Rindler-Ishak method [1], we shall apply it to the Janis-Newman-Winnicour (JNW) solution [2] deriving terms beyond the first order deflection and observe that they indeed coincide with the terms obtained by the known standard methods. Second one is the asymptotically non-flat Mannheim-Kazanas-de Sitter (MKdS) solution of Weyl gravity [3]. A special merit of this solution is that, it preserves the successes of Schwarzschild gravity on the local scale and explains flat rotation curve data *without* dark matter. Correction terms to Schwarzschild deflection due to halo gravity are enumerated. As a novel application of our result, we investigate how far the MKdS solution accounts for the matter decomposition (luminous+dark) of the Sloan Digital Sky Survey (SDSS) lens data obtained on board the Hubble Space Telescope (HST) [4].

We then discuss light deflection and weak gravitational lensing by the Ellis wormhole [5] including the one following from the Eddington-inspired-Born Infeld (EiBI) gravity [6]. Why wormholes? There are two reasons why we consider wormholes at all. First, such objects are valid solutions of Einstein's theory and have not yet been ruled out by observations. Second, and more important reason, there is a recent new result by Rahaman *et al* [7] that shows that galactic halo can support

wormholes. Thus, to get a feel of the deflection and lensing signatures of such exotic objects, we decided to devote later part of the work to this problem. Finally, we study the stability of Ellis and phantom wormholes [8] from a non-classical, prequantal statistical point of view developed by Tangherlini [9]. Below we describe the necessary ingredients for our work.

## 1.1 Brief history of light deflection

The only way we can obtain any information from distant astrophysical objects is through the passage of light signal from them to us. The intervening space is not vacuum but permeated by the gravitational field of the astrophysical object (in addition to dust and other materials, which we ignore here). One of the most important physical effect of the gravitational field is that it deflects the light rays from a background source passing by the gravitating astrophysical object. Although the experimental discovery of light deflection was made only in the last century, the possibility that there could be such a deflection had been suspected much earlier. Sir Issac Newton himself speculated that masses should deflect light but he did not describe the deflection properly, as he thought of light as only a wave phenomenon. Later on, other scientists and astronomers such as John Mitchell (1724-1793), Henry Cavendish (1731-1810) also studied the deflection of light and some calculations were done. Söldner (1804) also calculated the magnitude of the deflection by the sun using Newtonian theory. But these calculations yielded just one half of the true deflection observed today, because it was derived neglecting the local curvature of the spacetime around a massive object, a concept that was unheard of at that time.

Albert Einstein (1911) first realized that the deflection should be described by geodesic lines following the curvature of the spacetime. Thus the true deflection of light was obtained by Einstein (1915) using his full field equations of general relativity, a geometric theory based on curvature of 4D spacetime (3 space + 1 time), which is today regarded as a cornerstone of modern physics. According his formula, a light ray grazing the surface of the sun is deflected by  $\sim 1.75$  arcsec, which is twice the value compared to the previous Newtonian results. Møller [10] has clearly demonstrated how the factor of two arises: one half due to Newtonian theory in flat space and the other half due purely to the curvature of space. This accounts for the theoretical developments about light deflection.

On the experimental side, in 1919 a solar eclipse expedition in Sudan led by Sir Arthur Eddington, photographed stars in the vicinity of the sun. Comparing the eclipse photographs with photographs of the same stars taken few months earlier (when the intervening sun was absent) confirmed the deflection of the position of the star by an amount that Einstein calculated. This result brought the first experimental triumph of the theory of general relativity that revolutionized the then understanding of gravity. This deflection effect also introduced another concept: Since any gravitating object bends light just as any common glass lens does, that gravitating object could be regarded as a gravitational "lens". Use of the deflection equation in an appropriate gravitational lens equation, and study of the resulting observables, is what is commonly referred to as the phenomenon of gravitational lensing. For more details of the history of gravitational lensing, see Narayan *et al* [11].

Though Sir Arthur Eddington proved the bending of light rays by the sun taking photographs of the stars in 1919, and could easily be regarded as the precursor of gravitational lensing experiments, a more detailed experiment looking for observables such as image positions, magnifications etc., began with the discovery of Quasars in 1963. The first concrete example of gravitational lensing was observed in 1979 by discovering twin images QSO0957+561A,B separated by  $\sim 5.7$  arcsec at the same redshift  $z_s = 1.405$  and magnitude  $\approx 17$ . Following this discovery, more than a dozen of multiple-imaged Quasars are known till date. Therefore, gravitational lensing phenomenon is at the center stage of observational astrophysics. We outline it below. Throughout the thesis, we shall use units such that  $G = 1$ ,  $c = 1$ , unless specifically restored. Signature convention is  $(-, +, +, +)$ .

## 1.2 Basics of gravitational lensing

Gravitational lensing has become a very useful tool in astrophysics and cosmology today. This phenomenon is based on the effect of light deflection by gravity field, when light passes through the field. It is widely used to determine the cosmological constant, the distribution of dark matter and dark energy, the Hubble constant, the existence of extrasolar planet and so on (see e.g., Schneider *et al* [12]). If a light ray comes from  $-\infty$ , passes nearby an arbitrary spherical object of mass  $M$  at an impact parameter  $b$ , which is the perpendicular distance from the center of the mass to the asymptotic lines, and emerges at  $+\infty$ , then the light ray will be deflected by

a total angle (angle between the two asymptotes):

$$\alpha = \frac{4GM}{c^2b}, \quad (1.1)$$

where  $G$  is the Newton's gravitational constant and  $c$  is the speed of light in vacuum. If the light ray grazes the compact spherical mass, then  $b \sim$  radius of the spherical mass  $r_0 \sim$  closest approach distance  $R_0$ . The ray is still moving in the *weak field gravity* region because  $b \gg$  Schwarzschild radius  $\frac{2GM}{c^2}$ . An example is that the Schwarzschild radius of the sun is  $r_{\text{sch}} = \frac{2GM_{\odot}}{c^2} \sim 2.95$  km, while the present radius is  $r_0 \sim 700,000$  km, which evidently means that  $b \sim r_0 \gg r_{\text{sch}}$ . A simple geometry of light deflection is shown below, where the light path between the observer  $O$  and the source  $S$  is deflected by the mass  $L$ , which acts as a lens between them (Fig.1.1).

For example, if a light ray comes from a distant source and grazes the surface of the sun such that its impact parameter is equal to the sun's radius  $R_{\odot}$ , then one could take  $b \sim R_{\odot}$ , then the light ray is deflected by an angle

$$\alpha = \frac{4GM_{\odot}}{c^2R_{\odot}} \simeq 1.75 \text{ arcsec}, \quad (1.2)$$

which has been tested to a great accuracy ever since the early confirmation by the observation of Sir Eddington and his team in 1919. However, the spacetime we encounter to model other gravitational scenarios need not always be flat, and soon we shall be dealing with such a situation. We shall outline below a more general method, viz., that due to Rindler and Ishak [1], for calculating light deflection that can be applied even to asymptotically *non-flat* geometries. The expression for light deflection is crucial in the gravitational lens equation, which we outline below.

### 1.2.1 Lens Equation, Einstein Ring and Observables

Gravitational lens equation has been successfully employed to explain all the physical observables like magnification of images, double images from a single source etc, which Einstein had also mentioned in his notebook. Typical lensing geometry is given in Fig.1.1 below. The line joining the observer  $O$  and the lens  $L$  is taken as the optic axis.  $SQ$  and  $OI$  are the tangents to the null geodesics at the source ( $S$ ) and the image ( $I$ ) positions respectively;  $C$  is their point of intersection in absence of the lensing object  $L$ . The angular position of the source and the image are measured from the optic axis  $OL$ .  $\angle LOI$  (denoted by  $\vartheta$ ) and  $\angle LOS$  (denoted by  $\mathcal{B}$ ) are the

image and the source position respectively. A light ray from a source  $S$  is deflected by an angle  $\hat{\alpha}$  ( $\angle OCQ$ ) at the lens  $L$  and reaches an observer  $O$ . The distance between observer and lens, lens and source and observer and source are  $D_l$ ,  $D_{ls}$  and  $D_s$  respectively. Such distances are angular diameter distances. Perpendiculars  $LT$  and  $LN$  from  $L$  on the tangents  $OI$  and  $SQ$  represents the impact parameter  $b$ .  $r_0$  is the closest approach distance of the light ray from the lens.

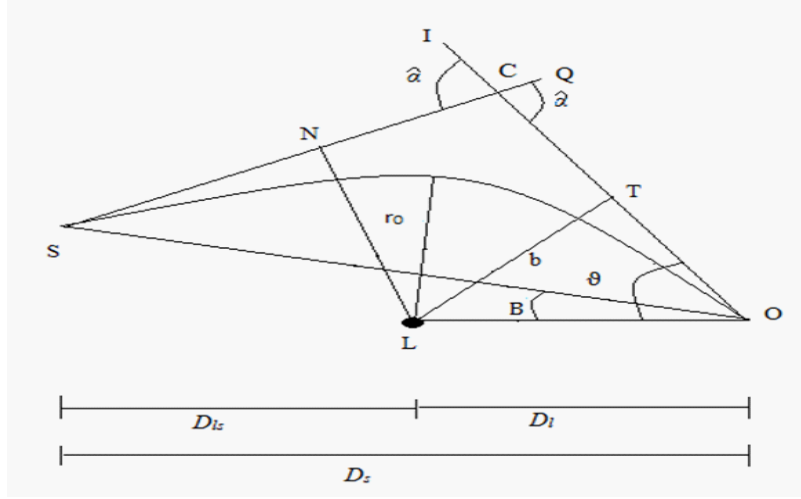


Fig.1.1. Geometry of a lensing system: A light ray from the source  $S$  is deflected by an angle  $\hat{\alpha}$  ( $\angle OCQ$ ) at the lens  $L$  and reaches an observer  $O$ .

Throughout the paper, we shall consider only the *thin lens approximation*, which means that the deflection occurs only at the point where the lens is, rest of the light trajectories on two sides of the lens are along straight lines. We start with a general lens equation [13], which relate the angular position of the source ( $\mathcal{B}$ ) and the image ( $\vartheta$ ), for deflection angle  $\hat{\alpha}$ :

$$\tan \mathcal{B} = \tan \vartheta - D \{ \tan \vartheta + \tan (\hat{\alpha} - \vartheta) \}, \quad (1.3)$$

where,  $D = \frac{D_{ls}}{D_s}$ .

We rescale the angular parameters as

$$\beta = \frac{\mathcal{B}}{\vartheta_E}, \quad \theta = \frac{\vartheta}{\vartheta_E}, \quad (1.4)$$

i.e., both  $\beta$  and  $\theta$  are the scaled angular positions of the source and image respectively. Here  $\vartheta_E$  is the weak deflection angular Einstein radius,

$$\vartheta_E = \sqrt{\frac{4mD}{d_l}}, \quad (1.5)$$

where  $m$  is the gravitational radius of lens,  $m = \frac{GM}{c^2}$  and  $M$  the physical mass.

Solution of the lens equation (1.3) can be written as a series expansion of the form [14],

$$\theta = \theta_0 + \theta_1 \varepsilon + \theta_2 \varepsilon^2 + \mathcal{O}(\varepsilon)^3, \quad (1.6)$$

where  $\theta_0$  is the image position in the weak deflection limit and the coefficients  $\theta_1$  and  $\theta_2$  are the first and second order correction terms respectively. The dimensionless parameter  $\varepsilon$  represents the angle subtended by the gravitational radius normalised by the Einstein radius  $\vartheta_E$ . This quantity is taken as expansion parameter and it is expressed as,

$$\varepsilon = \frac{\vartheta_E}{4D}. \quad (1.7)$$

With this substitutions, the lens equation becomes

$$\begin{aligned} 0 = & D \left[ -4\beta + \theta_0 - \frac{A_1}{\theta_0} \right] \varepsilon + \frac{D}{\theta_0^2} \left[ -A_2 + (A_1 + 4\theta_0^2) \theta_1 \right] \varepsilon^2 \\ & + \frac{D}{3\theta_0^3} \left[ -A_1^3 - 3A_3 + 12A_1^2 D \theta_0^2 - A_1 (56D^2 \theta_0^4 + 3\theta_1^2 - 3\theta_0 \theta_2) \right. \\ & \left. + 64D^2 \theta_0^3 (\theta_0^3 - \beta^3) + 6A_2 \theta_1 + 12\theta_0^3 \theta_2 \right] \varepsilon^3 + \mathcal{O}(\varepsilon)^4. \end{aligned} \quad (1.8)$$

We solve for  $\theta_0$ ,  $\theta_1$  and  $\theta_2$  by finding the values that make each term of the above lens equation (1.8) vanish. In this process we obtain,

$$\theta_0 = \frac{1}{2} \left( \beta + \sqrt{\beta^2 + A_1} \right), \quad (1.9)$$

$$\theta_1 = \frac{A_2}{A_1 + 4\theta_0^2}, \quad (1.10)$$

$$\begin{aligned}
\theta_2 = & \frac{1}{3\theta_0 (A_1 + 4\theta_0^2)^3} [A_1 \{-3A_2^2 + 3A_1A_3 - A_1^4 (D^2 - 1)\} \\
& + 4 \{-6A_2^2 + 6A_1A_3 + A_1^4 (D - 2)(D - 1)\} \theta_0^2 \\
& + 8 \{6A_3 + A_1^3 (2 + 11D^2 - 12D)\} \theta_0^4 \\
& + 64A_1^2 D (4D - 3) \theta_0^6 + 128A_1 D^2 \theta_0^8], \tag{1.11}
\end{aligned}$$

where  $A_1$ ,  $A_2$  and  $A_3$  are the coefficients of the invariant expressions of the bending angle [14]<sup>1</sup>. (1.6), (1.9), (1.10) and (1.11) together represents the image position  $\theta$  of the lensed images. It should be noted that for each  $\beta$  any source is imaged twice i.e., for  $\beta > 0$  we find the positive parity image  $\theta^+$  (primary) and for  $\beta < 0$  negative parity  $\theta^-$  (Secondary) and both images lies on the opposite side of the lens such that  $\theta^-(\beta) = \theta^+(-\beta)$ . For a particular value  $\beta = 0$ , we obtain the position of the Einstein ring.

The magnification  $\mu$  of a lensed image at angular position  $\vartheta$  is given by

$$\mu(\vartheta) = \left| \frac{\sin B(\vartheta) dB(\vartheta)}{\sin \vartheta \frac{dB(\vartheta)}{d\vartheta}} \right|^{-1}. \tag{1.12}$$

---

<sup>1</sup>For an isotropic form of spacetime metric given by,

$$ds^2 = A(r)dt^2 - B(r) \{dr^2 - r^2 (d^2\theta + \sin^2\theta d\varphi^2)\}.$$

the coefficients of the above metric in a PPN series upto third order is written as follows,

$$A(r) = 1 + 2\alpha_1 \left(\frac{\phi}{c^2}\right) + 2\gamma_1 \left(\frac{\phi}{c^2}\right)^2 + \frac{3}{2}\xi_1 \left(\frac{\phi}{c^2}\right)^3 + \dots,$$

$$B(r) = 1 - 2\delta_1 \left(\frac{\phi}{c^2}\right) + \frac{3}{2}\eta_1 \left(\frac{\phi}{c^2}\right)^2 - \frac{1}{2}\lambda_1 \left(\frac{\phi}{c^2}\right)^3 + \dots,$$

where  $\phi$  is the three-dimensional Newtonian potential with

$$\frac{\phi}{c^2} = -\frac{m}{r},$$

and  $\alpha_1$ ,  $\gamma_1$ ,  $\xi_1$ ,  $\delta_1$ ,  $\eta_1$  and  $\lambda_1$  denote the Eddington-Robertson parameters and they are so chosen that the Schwarzschild metric has  $\alpha_1 = \gamma_1 = \xi_1 = \delta_1 = \eta_1 = \lambda_1 = 1$ .

Finally the deflection angle is written in terms of the impact parameter  $b$  as,

$$\hat{\alpha}(b) = A_1 \left(\frac{m}{b}\right) + A_2 \left(\frac{m}{b}\right)^2 + A_3 \left(\frac{m}{b}\right)^3 + O\left(\frac{m}{b}\right)^4,$$

where the coefficients are

$$A_1 = 2(\alpha_1 + \delta_1),$$

$$A_2 = \left(2\alpha_1^2 - \gamma_1 + 2\alpha_1\delta_1 + \frac{3\eta_1}{4}\right) \pi,$$

$$A_3 = \frac{1}{3} [70\alpha_1^3 + 90\alpha_1^2\delta_1 - 36\gamma_1\delta_1 - 2\delta_1^3 + 9\delta_1\eta_1 - 60\alpha_1\gamma_1 - 18\alpha_1\delta_1^2 - 27\alpha_1\eta_1 + 3\lambda_1 + 9\xi_1].$$

After taking the derivative, we change to our scaled angular variables from Eqs.(1.4, 1.6), and substitute for  $\theta_1$  and  $\theta_2$  using Eq.(1.10) and Eq.(1.11). This yields a series expansion for the magnification,

$$\mu = \mu_0 + \mu_1\varepsilon + \mu_2\varepsilon^2 + \mathcal{O}(\varepsilon)^3, \quad (1.13)$$

where

$$\mu_0 = \frac{16\theta_0^4}{16\theta_0^4 - A_1^2}, \quad (1.14)$$

$$\mu_1 = -\frac{16A_2\theta_0^3}{(A_1 + 4\theta_0^2)^3}, \quad (1.15)$$

$$\begin{aligned} \mu_2 = & \frac{8\theta_0^2}{3(A_1 - 4\theta_0^2)(A_1 + 4\theta_0^2)^5} [-A_1^6 D_1^2 + 8A_1^2 \{6A_3 + A_1^3(2 + 6D - 9D^2)\} \theta_0^2 \\ & - 32 \{18A_2^2 - 12A_1A_3 + A_1^4(17D^2 - 12D - 4)\} \theta_0^4 \\ & + 128 \{6A_3 + A_1^3(2 + 6D - 9D^2)\} \theta_0^6 - 256A_1^2 D^2 \theta_0^8]. \end{aligned} \quad (1.16)$$

In case, the position of the primary and secondary images are close together to be extricable, total magnification and magnification-weighted centroid plays a vital role to study the gravitational lensing. Using our result we find the total magnification as,

$$\begin{aligned} \mu_{tot} &= |\mu^+| + |\mu^-|, \\ &= \frac{16A_1^2(\theta_0^8 - 1)}{(16\theta_0^4 - A_1^2)(A_1^2\theta_0^2 - 16)} - \frac{16(A_1 - 4)A_2\theta_0^3}{(A_1 + 4\theta_0^2)^3(4 + A_1\theta_0^2)^3} \\ &\quad [\{16 + A_1(4 + A_1)\}(\theta_0^6 - 1) + 12A_1\theta_0^2(\theta_0^2 - 1)]\varepsilon + \mathcal{O}(\varepsilon)^2. \end{aligned} \quad (1.17)$$

and magnification-weighted centroid as,

$$\Theta_{cent} = \frac{\theta^+ |\mu^+| + \theta^- |\mu^-|}{|\mu^+| - |\mu^-|}, \quad (1.18)$$

which can be written in terms of the expansion parameter  $\varepsilon$  as,

$$\Theta_{cent} = \Theta_0 + \Theta_1\varepsilon + \Theta_2\varepsilon^2, \quad (1.19)$$

where

$$\Theta_0 = \frac{\theta_0^+ \mu_0^+ + \theta_0^- \mu_0^-}{\mu_0^+ - \mu_0^-}, \quad (1.20)$$

$$\Theta_1 = \frac{\theta_1^- \mu_0^- + \theta_0^+ \mu_1^+ + \theta_0^- \mu_1^- + \theta_1^+ \mu_0^+}{\mu_0^+ - \mu_0^-}, \quad (1.21)$$

$$\Theta_2 = \frac{(\theta_0^+ + \theta_0^-)(\mu_0^+ \mu_2^- - \mu_0^- \mu_2^+) + (\mu_0^+ - \mu_0^-) [\mu_1^+(\theta_1^+ + \theta_1^-) + \theta_2^+ \mu_0^+ + \theta_2^- \mu_0^-]}{(\mu_0^+ - \mu_0^-)^2}. \quad (1.22)$$

The time delay of the lensed image is the difference between the light travel time for the ray when lens is absent, and the travel time for the ray, when the lens is present. It's expression in a series form is written as,

$$\tau = \tau_0 + \tau_1 \varepsilon + O(\varepsilon^2),$$

where

$$\begin{aligned} \tau_0 &= \frac{1}{2} \left[ \alpha_1 + \beta^2 - \theta_0^2 - \frac{A_1}{4} \ln \left( \frac{D_l \theta_0^2 \vartheta_E^2}{4D_{ls}} \right) \right], \\ \tau_1 &= \frac{A_2}{4\theta_0}. \end{aligned}$$

Since in our thesis, we shall be dealing with light deflection in the weak field approximation, a little more detail about what we mean by this is necessary.

### 1.2.2 Weak Field Approximation

Light moves far and near around any gravitating object. But how far is far and how near is near? In the spherically symmetric field of the lens, which is our interest here, the null geodesic produces a limiting sphere, called the photon sphere (defined explicitly later), that cannot be penetrated by light coming from outside the sphere. Since light cannot stop, it will continue to move on the photon sphere. However, it is an unstable sphere. If the light rays pass far from the photon sphere of the lens, then the deflection will be small and the lensing is said to be in the *weak field approximation*. But if the light rays pass very near to the photon sphere, then the deflection will be large and the lensing is said to be in the strong field approximation. Both kinds of lensing have become a well established tool for estimating the total mass of galaxies, galaxy clusters, their dark matter content and so on. The key information

about dark matter and dark energy can also be extracted from the signals of weak lensing. In the context of light motion in the galactic halo, what we mean by weak field approximation is that light rays may graze the luminous galactic mass, yet it would still be moving at a distance far away from the corresponding Schwarzschild mass, hence in the weak field regime [See the discussion after Eq.(1.1)].

Now a days, lots of analytical and numerical methods have been developed for calculating the deflection angle in weak deflection limit [11] for many astrophysical objects. Among these, we shall employ the Rindler-Ishak method [1], Keeton-Petters method [14] as well as some text book methods for comparison. Deflection in the weak field approximation has succeeded in explaining many astrophysical observations.

### 1.3 Galactic halo supports wormholes!

An intriguing and novel result has recently been proven: *Galactic halo spacetime can support wormholes* [7]. Therefore, for a better understanding of light motion in the galactic halo, it would be useful to get a feel of the light motion in the wormhole spacetimes. For this purpose, it is useful to provide a brief outline of this object. Wormholes are as good geometric solutions of Einstein's theory as are black holes – neither has been conclusively observed or ruled out to date. The predecessors of wormhole geometries are the Flamm paraboloid, Klein bottle or the early construction of the Einstein-Rosen two sheeted bridge etc.

By definition, a wormhole spacetime is a topological short-cut connecting two distant regions of a single spacetime or even two universes (Fig.1.2). The spacetime has to satisfy certain constraints, which we state using the Morris-Thorne [15] canonical form for the spacetime metric in “standard” coordinates, which is given by

$$d\tau^2 = -e^{2\Phi(R)}dt^2 + \left[1 - \frac{b(R)}{R}\right]^{-1} dR^2 + R^2(d\theta^2 + \sin^2\theta d\psi^2), \quad (1.23)$$

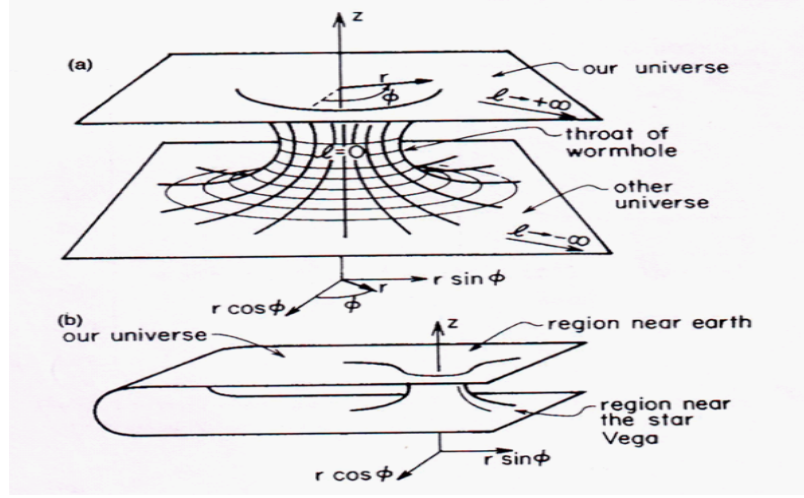


Fig.1.2. A typical wormhole geometry. (a) Embedding diagram for a wormhole that connects two different universes. (b) Embedding diagram for a wormhole that connects two distant regions of our own universe. Each diagram depicts the geometry of an equatorial ( $\theta = \frac{\pi}{2}$ ) slice through space at a specific moment of time ( $t = \text{constant}$ ).

Figures taken from Ref. [15].

where  $\Phi(R)$  and  $b(R)$  are redshift and shape functions, respectively, and  $R$  is defined by the positive circumferential radius  $2\pi R$ . The terminology for  $\Phi$  is self-evident. The space is spherical 3D at fixed time  $t$ . So without loss of information, we concentrate on the  $\theta = \pi/2$ ,  $t = \text{constant}$  2D slice in which the metric reads

$$d\tau^2 = \left[1 - \frac{b(R)}{R}\right]^{-1} dR^2 + R^2 d\psi^2. \quad (1.24)$$

We then remove the slice and embed it in the Euclidean 3D space having the metric

$$d\tau^2 = \left[1 + \left(\frac{dz}{dR}\right)^2\right] dR^2 + R^2 d\psi^2. \quad (1.25)$$

The isometry between (1.24) and (1.25) gives the shape of the axially symmetric

embedding surface  $z = z(R)$  obtained by integrating

$$\frac{dz}{dR} = \pm \left[ \frac{R}{b(R)} - 1 \right]^{-1/2}. \quad (1.26)$$

That is the reason why  $b(R)$  is called the shape function. However, in most natural situations and certainly in the Brans solutions, the integration does not yield expressions  $z = z(R)$  in a closed form. One would often need to plot the shape only by numerical calculation.

The basic constraints to be satisfied by a solution to qualify as a wormhole are as follows:

(a) The spacetime must have two asymptotically flat regions (mouths).

(b) The mouths must be connected by a throat defined by the minimum circumferential radius. This occurs at a place  $R = R_0$  where the vertical slope  $\frac{dz}{dR} = \infty$ . This implies that the throat radius  $R = R_0$  is a root of the equation  $b(R_0) = R_0$ . The wormhole has a hole of finite non-zero radius  $R_0 > 0$ , unlike a black hole center with zero radius. Thus,  $R \in [R_0, +\infty)$ .

(c) The shape function must satisfy:  $b(R)/R \rightarrow 0$  as  $R \rightarrow \infty$ . Also,  $b(R)/R \leq 1$  for all  $R \geq R_0$ .

In order that the wormhole indeed flares out to two asymptotically flat spacetimes, the following condition

$$\frac{d^2R}{dz^2} = \frac{b - b'R}{2b^2} > 0 \quad (1.27)$$

must be satisfied at or near the throat. This inequality imposes a constraint on the type of source stress tensor  $\mathbf{T}_{\mu\nu}$ . Assuming an isotropic scalar field stress tensor  $\mathbf{T}_{\hat{\mu}\hat{\nu}}^{(\varphi)} = [\rho, p_R, p_\theta, p_\psi]$  in the static local orthonormal frame ( $\hat{\cdot}$ ), the left hand side of vacuum Brans-Dicke field equations  $\mathbf{R}_{\hat{\mu}\hat{\nu}} - \frac{1}{2}\eta_{\hat{\mu}\hat{\nu}}\mathbf{R} = \mathbf{T}_{\hat{\mu}\hat{\nu}}^{(\varphi)}$  straightforwardly yield

$$\rho = b'/R^2, p_R = [2(R-b)\Phi' - b/R]/R^2, p_\theta = p_\psi = p_R + (R/2)[(\rho + p_R)\Phi' + p'_R], \quad (1.28)$$

where primes denote differentiation relative to radius  $R$ ,  $\rho$  is the scalar field energy density,  $p_R$  is the radial tension,  $p_\theta, p_\psi$  are transverse pressures, and  $\eta_{\hat{\mu}\hat{\nu}}$  is the Minkowski metric in the orthonormal frame. Then the inequality in Eq.(1.27) can be nicely rephrased by using the Morris-Thorne [15] function  $\zeta$  defined by  $\zeta = -\frac{\rho + p_R}{|\rho|}$ . Putting in it the expressions from Eq.(1.28), combining it with the equality in Eq.(1.27) and noting that  $(R - b)\Phi' \rightarrow 0$  at  $R = R_0$ , we get at the throat the

following result

$$\zeta = \frac{2b^2}{R|b'|} \frac{d^2R}{dz^2} = - \left( \frac{\rho + p_R}{|\rho|} \right), \quad (1.29)$$

which shows that the flaring out condition (1.27) is satisfied only if  $\rho + p_R < 0$ . This violates a known energy condition since, for normal matter,  $\rho + p_R > 0$  (null energy condition). A fast Lorentz boosted traveller might see the violation as  $\rho < 0$ , which means a violation of the weak energy condition. Such energy condition violating matter is called “exotic”. Thus the flaring out constraint suggests that:

(d) We must have:  $\rho < 0$  and/or  $\rho + p_R < 0$  at least at or near the throat.

(e) There should be no horizon, that is, the redshift function  $\Phi$  must be finite everywhere to prevent infinite redshift of signals from the traveller to outside stationary observer.

(f) The tidal forces (that are proportional to curvature tensor) experienced by a traveller should be finite throughout the trip and the travel time from one mouth to the other should be reasonable (traversability conditions).

These are the main constraints to be satisfied if a given spacetime has to represent a regular wormhole, traversable in principle. Practical traversability by humans further requires that the tidal forces be tolerable, that is, it should be of the order of one Earth gravity. However, not all wormholes are traversable due to the occurrence of singularity or horizon in the spacetime.

## 1.4 Objectives

The broad objective of this thesis is to present several new results emanating from the study of light motion in the galactic halo described by the MKdS solution of Weyl gravity and in wormhole spacetimes in the weak field limit. Why wormholes? Because, recently, it has been shown that galactic halo spacetime can support wormholes [7]. Therefore, to understand light motion in the galactic halo, it is necessary to understand light motion in a wormhole spacetime. Hence, later part of the thesis will be devoted to presenting some interesting results of light motion in the wormhole spacetimes, notably the Ellis wormhole of Einstein Minimally coupled Scalar field (EMS). A generalization of the Ellis wormhole is available in the Einstein-inspired-Born-Infeld (EiBI) gravity characterized by a parameter  $\kappa$  [6]. We shall study its effect on various physical observables. Stability of Ellis wormhole is studied from an

interesting and novel angle using an approach developed by Tangherlini [9]. Chapterwise objectives are as follows:

- To test the validity of the Rindler-Ishak method for light deflection used in the thesis, we shall derive the expression for light bending up to second order in the well known Janis-Newman-Winnicour (JNW) spacetime [2] of EMS theory. We shall confirm the expression for bending by using two different text book methods viz., perturbation method and integration method. As a by-product, we shall analyze the stability of circular orbits in the JNW solution using autonomous Hamiltonian dynamical system [17] illustrating its dependence on the JNW parameter  $\zeta$  (**Chapter 2**).
- We shall adopt Rindler-Ishak method [1] to study light motion in the galactic halo modelled by MKdS solution of Weyl gravity. The solution containing a halo parameter  $\gamma$  is more general than the SdS spacetime. Dealing appropriately with the light motion in the weak field regime, we shall find exactly how light bending is affected by the halo parameter  $\gamma$ . Previous result on deflection in the literature concerning the effect of  $\gamma$  is modified (**Chapter 3**).
- The photometric and spectroscopic data available from the Sloan Digital Sky Survey (SDSS) lens data have been analyzed in the literature determining the luminous and dark matter compositions in the selected early-type sample of 57 lens galaxies [16]. Applying the expression for light bending derived in the previous chapter, we wish to investigate how far the MKdS solution of Weyl gravity accounts for the matter decomposition of the SDSS galaxies (**Chapter 4**).
- We shall calculate the gravitational lensing observables associated with the traversable EMS class II wormhole made of a ghost field by employing a post-post-Newtonian (PPN) method developed by Keeton and Petters [14] (**Chapter 5**).
- We shall analyze the effects of the parameter  $\kappa$  present in the wormhole solution of the EiBI gravity theory on various physical effects (**Chapter 6**).
- We shall re-examine the stability of Ellis wormhole and also of phantom wormholes by finding their probability using a non-classical, prequantal statistical

simulation of reflectivity and transmissivity coefficients developed by Tangherlini [9]. We shall adapt Tangherlini's approach to effective medium and combine it with Hamilton's optical mechanical analogy [18] to reach our goal (**Chapter 7**).

- Finally, we shall summarize the obtained results of the thesis (**Chapter 8**).

## 1.5 Methodologies

We shall mainly adopt the following methodologies to realize the above mentioned objectives:

- To calculate the light bending angle, we shall adopt the recently developed invariant angle method given by Rindler and Ishak [1], which can be equally applied to asymptotically flat and nonflat spacetimes. In fact, it can be applied to any static spherically symmetric metric. Also we shall employ the standard text book methodology, viz., the direct integration method and perturbation method to confirm the bending expression obtained by Rindler-Ishak method.
- We shall adopt a physical principle, viz., interpret the Weyl angle to be the same as the Einstein angle for a light ray with the same impact parameter. This is equivalent to saying that the *observed angle* must be the same as the predicted one, whatever be the theory. This will be a new input for calculating the mass decomposition (luminous+dark) in galaxies.
- To calculate the stability of circular orbits, we shall apply the method of autonomous Hamiltonian dynamical system [17].
- We shall employ the method developed by Keeton and Petters [14] to calculate the bending angle in the weak deflection approximation. This method is based on the PPN formalism, where the deflection angle and lensing observables are obtained by expansion of the lens equation as a perturbation series solution.
- Using Tangherlini's method of non-classical, prequantal statistical simulation [9], in combination with Hamilton's optical mechanical analogy, we shall re-examine the stability of Ellis and phantom wormhole.

## 1.6 Organisation of the contents

The contents are organized as follows: Apart from the Introductory Chapter 1, this thesis comprises of 7 more chapters. In Chapter 2, we shall test the validity of the Rindler-Ishak method using the JNW spacetime. Then we apply the method to deal with the light bending in weak field approximation in the galactic halo described by the MKdS solution of Weyl gravity (Chapter 3). We shall apply the result to decompose the galactic halo mass into luminous+dark matter and compare it with the simulations based on the SDSS data (Chapter 4). In view of the new fact that galactic halo can support wormholes, we shall deal with light motion and their stability analysis in some known wormholes in the next three Chapters (5,6,7). In the last Chapter (8), we shall summarise the results obtained in this thesis.

The individual chapters are organized as follows: Each chapter includes introduction, main body, conclusion and the references used in the chapter, i.e., each chapter is made complete in itself. Hence a bit of repetition of some references might unavoidably occur. This is done only to help easy readability. In the very beginning of the thesis, we provide a detailed list of figures and of tables that would follow in the body of the thesis, which will be very helpful for the readers to locate the respective items. We have also provided a page index at the very end of the thesis.

## 1.7 References

- [1] W. Rindler and M. Ishak, Phys. Rev. **D 76**, 043006 (2007).
- [2] A. I. Janis, E. T. Newman and J. Winicour, Phys. Rev. Lett. **20**, 878 (1968).
- [3] P. D. Mannheim and D. Kazanas, Astrophys. J. **342**, 635 (1989); P. D. Mannheim, Astrophys. J. **479**, 659 (1997); P. D. Mannheim, Phys. Rev. D **75**, 124006 (2007). See also the review: P.D. Mannheim, Prog. Part. and Nucl. Phys. **56**, 340 (2006).
- [4] A.S. Bolton, S. Burles and L.V.E. Koopmans *et al*, Astrophys. J. **682**, 964 (2008).
- [5] H. Ellis, J. Math. Phys. **14**, 104 (1973).
- [6] M. Bañados and P.G. Ferreira, Phys. Rev. Lett. **105**, 011101 (2010).
- [7] F. Rahaman, P.K.F. Kuhfittig, S. Ray and N. Islam, Eur. Phys. J. C **74**,

- 2750 (2014).
- [8] F.S.N. Lobo, Phys. Rev. D **71**, 084011 (2005).
  - [9] F.R. Tangherlini, Phys. Rev. A **12**, 139 (1975).
  - [10] C. Møller, *The Theory of Relativity*, 2nd ed. (Oxford University, Oxford, 1972), pp.498-501.
  - [11] R. Narayan and M. Bartelmann, 1996, *Lectures on gravitational lensing*, astro-ph/9606001.
  - [12] P. Schneider, J. Ehlers and E. E. Falco, *Gravitational Lenses* (Springer-Verlag, Berlin, 1992).
  - [13] K. S. Virbhadra, D. Narasimha, and S. M. Chitre, Astron. Astrophys. **337**, 1 (1998); K. S. Virbhadra and G. F. R. Ellis, Phys. Rev. **D 62**, 084003 (2002).
  - [14] C. R. Keeton and A.O. Petters, Phys. Rev. D **72**,104006 (2005); *ibid.* **D 73**, 044024 (2006); *ibid.* **D 73**, 104032 (2006).
  - [15] M. S. Morris and K. S. Thorne, Am. J. Phys. **56**, 395 (1988).
  - [16] C. Grillo, R. Gobat, M. Lombardi and P. Rosati, Astron. Astrophys. **501**, 461 (2009).
  - [17] D. W. Jordan and P. Smith, *Non linear ordinary differential equation*, 3rd edition (Oxford University press, Oxford, 1999); For an application to gravity, see: A. Palit, A. Panchenko, N. G. Migranov, A. Bhadra and K. K.Nandi, Int. J. Theor. Phys. **48**, 1271 (2009).
  - [18] A. González, F.S. Guzmán and O. Sarbach, Class. Quant. Grav. **26**, 015010 (2009); Class. Quant. Grav. **26**, 015011 (2009).
  - [19] K.K. Nandi and A. Islam, Amer. J. Phys. **63**, 251 (1995).
-